Design Formulas for Planar Fabry–Pérot Cavity Antennas Formed by Thick Partially Reflective Surfaces

Alister Hosseini, Franco De Flaviis, and Filippo Capolino

***Abstract*— Simple closed-form formulas are proposed to estimate the broadside radiation performance of planar Fabry–Pérot-cavity (FPC) antennas formed by an arbitrary thick partially reflective-surface (PRS). The new formulas also estimate the attenuation and propagation constant of the leaky waves excited in the FPC when covered by such a thick PRS. When the PRS thickness vanishes the derived formulas reduce to those previously derived for FPC formed by infinitesimally thin PRS. Notably, we demonstrate that the same fundamental limit for the figure of merit defined as the pattern bandwidth-directivity product holds, as that for FPC with thin PRS, under the approximation that the phase variation of the PRS scattering parameters is not too rapid. The accuracy of the proposed formulas is verified with comparisons to numerical full-wave simulations.**

***Index Terms*— Leaky-wave (LW) antenna, planar Fabry–Pérot-cavity (FPC) antenna formed by a thick partially reflective-surface (PRS), simple design formulas.**

I. Introduction

Planar Fabry–Pérot-cavity (FPC) antennas, a class of leaky-wave (LW) antennas [1]–[22], are known as a promising solution to produce highly efficient directive radiation using a single feed point. This antenna consists of a grounded cavity formed by using a partially reflective-surface (PRS) superstrate. In [9]–[13], [19], and [20], few designs of fully or partially air-filled FPCs formed by a thick PRS are proposed. The thickness of PRS may be necessary in some applications for practical reasons or even unavoidable at millimeter waves because of the short wavelength. FPC antennas whose PRS is formed by a *thin* frequency-selective-surface (FSS), were discussed in [1], [2], [5]–[8], and [14]–[18]. A *thin* PRS, where the thickness of the PRS is much smaller than the wavelength at the resonance frequency of the cavity, is simply modeled as shunt admittance, which is purely imaginary when metallic losses are negligible. On the other hand, when the thickness of a PRS becomes comparable to the operating wavelength of the antenna, e.g., at very high frequencies as in [9]–[13], [19], and [20], or when the PRS has to be mechanically stable so its thickness is increased, a simple shunt susceptance cannot model the PRS anymore and a two port network is necessary as in Fig. 1.

Although samples of FPC antennas, formed by a thick PRS, were discussed in [9], [19], [20], and [22], the general radiation performance of such cavities has not been sufficiently studied yet. Here, novel simple formulas are proposed estimating the resonance condition, the 3 dB gain bandwidth (GBW), 3 dB beamwidth, and maximum directivity of such FPC antennas as a function of the effective susceptance and conductance of the PRS used in the simplified transmission-line (TL) circuit model of the cavity. The values of the properties described in this communication obtained from the proposed formulas are compared to both numerical (i.e., calculated analytically based on the TL model of the antenna) and full-wave (FW) numerical results.

Manuscript received March 30, 2015; revised August 24, 2016; accepted September 6, 2016. Date of publication September 13, 2016; date of current version December 5, 2016.

The authors are with the Department of Electrical Engineering and Computer Sciences, University of California at Irvine, Irvine, CA 92697 USA (e-mail: alister.hosseini@gmail.com; franco@uci.edu; f.capolino@uci.edu).

Color versions of one or more of the figures in this communication are available online at http://ieeexplore.ieee.org.

Digital Object Identifier 10.1109/TAP.2016.2608934

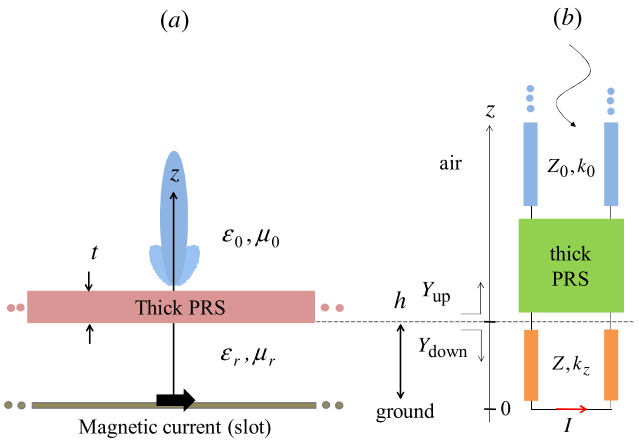

Fig. 1. (a) General FPC antenna geometry with thick PRS excited with a magnetic current on its ground plane (i.e., a slot). (b) Equivalent TL model of an FPC antenna formed by a thick PRS modeled with a two-port network. By using reciprocity radiation is evaluated by determining the current I, varying either frequency or pointing angle.

II. Radiation Performance of FPCs Using a Thick PRS

Aiming at describing near-broadside radiation performance of FPC antennas (i.e., along the z-direction, covering very small beam tilts around the z-axis) as in [1], [2], and [5]–[8], we adopt the equivalent TL model in Fig. 1 based on the transverse equivalent network. Accordingly, electric and magnetic fields are modeled by equivalent voltages and currents, respectively [23]. An ideal magnetic current (representing a slot on the cavity-ground), is used to excite the antenna. Furthermore, by using reciprocity the far field radiated by an elementary magnetic dipole source $J_m = 1$ Vm on the cavity ground plane as in Fig. 1(a) is related to the current I generated by an incoming voltage wave as shown in Fig. 1(b) and described in [1], [2], [5]–[8], [16], [17], and [24].

In the TL model of the antenna, shown in Fig. 1, free-space above the cavity is modeled as an infinite-length TL with free-space characteristic wave impedance. Based on simplifications, valid for highly directive FPCs as also discussed in [1], for small angle of radiation, in transmission mode, or small angle of plane wave incidence, in reception mode, the characteristic wave impedance of TE and TM waves can be approximated with that of a TEM wave $Z_0 = 1/Y_0 = (\mu_0/\varepsilon_0)^{1/2}$. Similarly, the cavity whose material is described by the constitutive relative parameters ε_r and μ_r, is modeled as an equivalent TL with length h, with quasi TEM characteristic impedance $Z = Z_0/\xi_r$ where $\xi_r = (\varepsilon_r/\mu_r)^{1/2}$ and $Z = Z_0(\mu_r/\varepsilon_r)^{1/2}$. (Subsequent evaluation of LWs, instead, requires the distinction between TE and TM LWs.) The longitudinal TL wavenumber inside the cavity is $k_z = k_0(\varepsilon_r\mu_r - \sin^2\theta)^{1/2}$, with $k_0 = \omega/c$ and $c = 1/(\varepsilon_0\mu_0)^{1/2}$ is speed of light in free-space. The TL describing the reception mode is terminated on a short circuit (the ground).

For electrically *thick* PRSs, the thin-PRS-model used in [1], [2], and [5]–[8] cannot be used. Referring to Fig. 1, we use a two-port network model for a thick PRS as in [19]. Looking at the TL model shown in Fig. 1, the upward and downward admittances at the bottom interface of the PRS are denoted by $Y_{up} = Y_0(\hat{g} + j\hat{b})$ and $Y_{down} = -j\xi_r Y_0 \cot(k_z h)$, respectively.

Strictly speaking, these values depends also on the angle of incidence (or radiation), however, for the case of near broadside

characterization we can assume that these values are determined for normal incidence. (For what concerns LWs calculations, instead, a distinction will be made for TE and TM LWs.) Without providing details that have been already shown elsewhere [16], [17], [24], based on reciprocity and the TL model in Fig. 1, the radiated power density at and near broadside direction of the antenna is expressed as

$$P(\omega,\theta)\cong\frac{P^{+}}{\sin^{2}(k_{z}h)}\left(\frac{\hat{g}}{\hat{g}^{2}+(\hat{b}-\xi_{r}\cot(k_{z}h))^{2}}\right) \tag{1}$$

where P^{+} is a constant calculated using reciprocity theorem as extensively discussed in [1] and [16]–[18]. However, for clarity, we recall that in order to derive (1), the following simplification steps, valid for highly directive FPC antennas, have been considered.

1) Based on discussions in previous analytical studies, as in [1], for highly directive FPC antennas, the φ-dependency of the power density formula is negligible when looking at the field in the broadside region.
2) The characteristic wave impedances/admittances, varying θ, should be expressed in their TE/TM formats (as discussed in [24]), however, for highly directive FPCs and for small values of θ, the respective values converge to their TEM forms.
3) It is assumed that for the highly directive FPCs and for small values of θ, around broadside, both $\hat{b}$ and $\hat{g}$ remain unchanged with respect to θ.
4) We have considered a lossless PRS in the derivation of the simple formula (1). If the PRS has losses, the power density near broadside would have a slightly more complicated expression than that in (1).

At broadside (i.e., $\theta=0$ or along z-axis), (1) converges to

$$P=\frac{P^{+}}{\sin^{2}(kh)}\left(\frac{\hat{g}}{\hat{g}^{2}+Z_{0}^{2}B_{\text{tot}}^{2}}\right) \tag{2}$$

where $B_{tot}=\text{Im}(Y_{\text{up}}+Y_{\text{down}})=Y_{0}(\hat{b}-\xi_{r}\cot kh)$ is the imaginary part of the total admittance of the antenna $Y_{\text{up}}+Y_{\text{down}}$ where $k=k_{0}(\varepsilon_{r}\mu_{r})^{1/2}$. To find the resonance height of the antenna h, the total imaginary admittance of the antenna, at the radian resonance frequency ω_{res}, must be set to zero, i.e., $B_{\text{tot}}(\omega_{\text{res}})=0$. This leads to

$$\cot(hk_{\text{res}})=\hat{b}/\xi_{r} \tag{3}$$

where $k_{\text{res}}=\omega_{\text{res}}/v$ and $v=1/(\varepsilon_{r}\varepsilon_{0}\mu_{r}\mu_{0})^{1/2}$ is speed of light inside the cavity. It is notable that the radiation power density (2) is a function of both $\hat{b}$ and $\hat{g}$. Dealing with highly directive FPC antennas with thick PRS, and considering $\cos(hk_{\text{res}})\cong 1$ in (3) for such cavities, the maximum broadside radiation power density occurs in proximity of the resonance frequency and it has the expression

$$P_{\max}\cong P_{\text{res}}=\frac{P^{+}}{\sin^{2}(hk_{\text{res}})}\left(\frac{1}{\hat{g}}\right)\approx P^{+}\frac{\hat{b}^{2}}{\hat{g}\xi_{r}^{2}}. \tag{4}$$

A. Power Bandwidth Formula

The radiated broadside power density (2) of the antenna is used to estimate the 3 dB power bandwidth (PBW) of the antenna defined as the frequency interval within which the broadside power density remains within the -3 dB range of its maximum value $P_{\max}$. Note that the PBW of the antenna is useful to estimate the 3 dB GBW of the antenna. Using the power density equation (2), the PBW of this FPC antenna is found as $\text{PBW}=(\omega_{3dB}^{+}-\omega_{3\text{ dB}}^{-})/\omega_{\text{res}}$. The upper and lower radian frequencies $\omega_{3\text{ dB}}^{\pm}$ are found by solving

$$P(\omega_{3\text{ dB}}^{\pm})=\frac{P_{\max}}{2}\cong\frac{P_{\text{res}}}{2}. \tag{5}$$

For highly directive FPCs, it is assumed with good approximation that the frequency variation of $\hat{b}$ and $\hat{g}$ is negligible around the resonance frequency of the cavity. Henceforth, in the following both $\hat{b}$ and $\hat{g}$ are evaluated at or in proximity of the FPC resonance frequency. Following formulas [16, eqs. (9)–(11)], and using (2)–(4), the normalized PBW of an FPC formed by using a thick PRS is estimated using (5). For highly directive FPC antennas one has $|\hat{b}|\gg 1$, as it will be discussed in the next section, and $\hat{b}^{4}$ is the dominant term in (5). Moreover, using (3) with $|\hat{b}|\gg 1$, one has $v/h\cong\omega_{\text{res}}/\pi$. Therefore, the normalized PBW of the antenna is further simplified as

$$\text{PBW}\cong\left(\frac{v}{h}\right)\frac{2\hat{g}\xi_{r}}{\omega_{\text{res}}}\frac{\sqrt{2\hat{g}^{2}\hat{b}^{2}+\left(\hat{b}^{2}+\xi_{r}^{2}\right)^{2}}}{\hat{g}^{2}\hat{b}^{2}+\left(\hat{b}^{2}+\xi_{r}^{2}\right)^{2}}\cong\frac{2\hat{g}\xi_{r}}{\pi\hat{b}^{2}}. \tag{6}$$

B. Beamwidth and Maximum Directivity

A planar FPC antenna has a directive radiation pattern along the z-axis ($\theta=0$) as shown in Fig. 1, in the proximity of its resonance frequency. The 3 dB beamwidth is defined as the angular range within which the radiated power density from the antenna remains within -3 dB range of its maximum value at broadside ($\theta=0$) at its resonance frequency. The 3 dB angle ($\theta_{3\text{ dB}}$) of the radiation pattern of the antenna (at ω_{res}) is found from the following equation:

$$P(\omega_{\text{res}},\theta_{3\text{ dB}})=\frac{P_{\max}}{2}\cong\frac{P(\omega_{\text{res}},\theta=0)}{2}. \tag{7}$$

In general the PRS filtering property depends in the angle of incidence, however, for highly directive FPC antennas, $\theta_{3\text{ dB}}\ll\pi$; therefore, it is assumed that the values of both $\hat{b}$ and $\hat{g}$ remains unchanged. At the direction $\theta_{3\text{ dB}}$, the radiation power density is approximated using (1), where the term outside the parenthesis $\sin^{2}hk_{z}\cong\sin^{2}hk_{\text{res}}$ for $\theta_{3\text{ dB}}\ll\pi$, whereas $k_{z\theta_{3\text{ dB}}}=k_{0,\text{res}}(\varepsilon_{r}\mu_{r}-\sin^{2}\theta_{3\text{ dB}})^{1/2}$ for the term inside the parenthesis. Solving (7) and considering $\sin\theta_{3\text{ dB}}\cong\theta_{3\text{ dB}}$, results in

$$\left|\hat{b}-\xi_{r}\cot\left(hk_{0,\text{res}}\sqrt{\varepsilon_{r}\mu_{r}-\theta_{3\text{ dB}}^{2}}\right)\right|=\hat{g}. \tag{8}$$

Using approximations $(1-\Delta)^{1/2}\cong 1-\Delta/2$ and $\cot(x_{0}+\Delta)\cong\cot(x_{0})-\Delta/\sin^{2}(x_{0})$, for small values of Δ, solving (8) results in $\theta_{3\text{ dB}}^{2}=2\varepsilon_{r}\mu_{r}\hat{g}\sin^{2}(hk_{\text{res}})/(\xi_{r}k_{\text{res}}h)$. Using [16, eq. (11)], and considering $k_{\text{res}}h\cong\pi$, the $\theta_{3\text{ dB}}$ of a directive FPC antenna formed by a thick PRS is expressed as

$$\theta_{3\text{ dB}}\cong\frac{1}{|\hat{b}|}\sqrt{\frac{2\varepsilon_{r}\mu_{r}\xi_{r}\hat{g}}{\pi}}. \tag{9}$$

In our case relative to thick PRSs, by increasing $\hat{b}$and/or decreasing $\hat{g}$, the 3 dB angle (9) of radiation pattern of the antenna decreases corresponding to a higher directivity. For highly directive FPC antennas, the 3 dB beamwidth of the main beam is almost equal in both E- and H-planes being expressed as $\Delta\theta_{E}\cong\Delta\theta_{H}\cong 2\theta_{3\text{ dB}}$. Following [25, eq. (2.27)], the maximum directivity of the antenna is estimated as $D_{\max}\cong\pi^{2}/(\Delta\theta_{E}\times\Delta\theta_{H})$ which, using (9), is expressed as

$$D_{\max}\cong\frac{\pi^{3}\hat{b}^{2}}{8\varepsilon_{r}\mu_{r}\xi_{r}\hat{g}}\cong 3.9\frac{\hat{b}^{2}}{\varepsilon_{r}\mu_{r}\xi_{r}\hat{g}}. \tag{10}$$

III. Leaky-Wave Analysis

The radiation performance of FPC antennas is explained based on two dominant TE and TM LWs excited in the FPC [1], [8] and propagating (i.e., leaking power) radially with attenuation and propagation constants, α and β, respectively. Similar to [1], the

dispersion relation of the LW transverse complex wavenumbers $k_t = \beta - j\alpha$ of the dominant TE and TM LWs in the FPC versus frequency, is found by solving

$$Y_{\text{tot}}^{\text{TE/TM}}(k_t) = Y_{\text{up}}^{\text{TE/TM}}(k_t) + Y_{\text{down}}^{\text{TE/TM}}(k_t) = 0. \tag{11}$$

Here, k_t denotes the transverse complex wavenumber of a radially propagating mode in the xy plane. Based on Fig. 1, $Y_{\text{up}}^{\text{TE/TM}}$ and $Y_{\text{down}}^{\text{TE/TM}}$ are evaluated by using the TE and TM characteristic impedances as defined in [1] that are functions of k_t (in contrast to the formulas in the previous section where the characteristic impedances are those for a TEM wave).

The "optimum" radiation condition $\alpha \cong \beta \ll k_{\text{res}}$ for each dominant TE and TM wave, as discussed in [1] and [20], occurs at distinct (but close to each other) frequencies denoted as f_{TE} and f_{TM}, for TE and TM waves, respectively. However, for very directive FPC antennas radiating broadside, the optimum condition $\alpha \cong \beta \ll k_{\text{res}}$ occurs for both TE and TM LWs when $f_{\text{TE}} \cong f_{\text{TM}} \cong f_{\text{res}}$, i.e., approximately at the same frequency, as it will be shown in the next section and as discussed also in [1] and [14]. Instead, for moderately low-gain FPC antennas, f_{TE} and f_{TM} are slightly shifted. Looking at $k_t = \beta - j\alpha$, at the optimum condition one has $\hat{\beta} = \hat{\alpha} = \delta$ where δ is a small positive number, and $\hat{\beta} = \beta/k_{\text{res}}$ and $\hat{\alpha} = \alpha/k_{\text{res}}$ are both much smaller than unity. By replacing $\hat{\beta} = \hat{\alpha} = \delta$ into (11), at ω_{res}, the dispersion equation (11) is approximated as

$$j\left(\hat{b} - \xi_r \cot\left(hk_{\text{res}}\sqrt{1 + \frac{2j\delta^2}{\varepsilon_r\mu_r}}\right)\right) + \hat{g} = 0. \tag{12}$$

Considering that $B_{\text{tot}}(\omega_{\text{res}}) = 0$ and using the approximations already discussed before (9), the dispersion relation (12) yields to an approximate expression for δ, and the LW attenuation and propagation constants of both dominant TE and TM waves are estimated by

$$\hat{\alpha} = \hat{\beta} = \delta \cong \frac{\sqrt{\hat{g}}}{|\hat{b}|}\sqrt{\frac{\mu_r\varepsilon_r\xi_r}{\pi}} = \frac{\sqrt{\hat{g}}}{|\hat{b}|}\sqrt{\frac{\mu_r^{0.5}\varepsilon_r^{1.5}}{\pi}}. \tag{13}$$

IV. Discussion

Looking at the derived formulas, the following observations are summarized.

1) From (2), the maximum radiated power density can be achieved not only by having a large absolute value of $\hat{b}$ but also by decreasing $\hat{g}$. This implies that the cavity height of the antenna can be finely tuned by modifying $\hat{b}$, and independently controlling the radiation gain with $\hat{g}$. This is important when standard cavity heights are based on using commercial substrates in practical implementations of FPCs.
2) The *figure of merit* (FoM) for a highly directive FPC formed by a thick PRS is defined, analogously to that for FPCs formed by a thin PRS discussed in [7] and [8], by the product of the maximum directivity and the PBW. Using (6) and (10), the FoM for the case of an FPC with *thick* PRS is expressed as

$$\text{FoM} = D \times \text{PBW} = \frac{\pi^2}{4\varepsilon_r\mu_r} \cong \frac{2.47}{\varepsilon_r\mu_r} \tag{14}$$

which is remarkably the same as that for FPC antennas with thin FSS discussed in [7] and [8]. Note that in this analysis we have assumed parameters $\hat{g}$ and $\hat{b}$ do not vary significantly with frequency. And it must be noted that a thick PRS may also imply that in specific cases a more complicated frequency dispersion of $\hat{g}$ and $\hat{b}$ than those considered here, in particular due to involved PRS resonances. This would induce a more complex frequency behavior of D and a different PBW than those in [7] and [8] may occur that may lead to wideband FPC antenna operations. This would require better approximations than those in (6) and (10) that may lead to larger values of the FoM. Such more accurate formulas should be derived based also on the discussions reported in [17] and [18], and should not being based only on the leading order of the Taylor expansions used in the previous sections.
3) For a *thin* PRS one has $\hat{g} \cong 1$; therefore, all the proposed formulas in this section reduce to formulas described in [1], [2], and [5]–[8], for a high-gain FPC antenna formed by a *thin* PRS (i.e., the newly derived formulas (6), (9), and (13) here, for $\hat{g} \cong 1$, converge to formulas (33), (36), and (24), in [1], respectively).
4) Simple substitutions in (4), (6), (9), (10), and (13), lead to the following expressions, all functions of the LW constant δ:

$$\begin{aligned} P_{\max} &\cong P^{+}\frac{\varepsilon_r\mu_r}{\pi\xi_r\delta^2} \\ \text{PBW} &= \frac{2}{\varepsilon_r\mu_r}\delta^2 \\ \Delta\theta_E &\cong \Delta\theta_H \cong 2\theta_{3\text{ dB}} \cong 2\sqrt{2}\delta = 2.83\delta \\ D_{\max} &\cong \frac{1}{\delta^2}\frac{\pi^2}{8} \cong \frac{1.23}{\delta^2}. \end{aligned} \tag{15}$$

5) These formulas are identical to those in [1], [2], [7], and [8] for FPC antennas with thin PRSs, and show that the FPC antenna radiation performance depends on a single parameter, the LW attenuation constant, when working at the so called optimum condition $\hat{\beta} = \hat{\alpha} = \delta$, even in the case of thick PRS.
6) By including the frequency variations of $\hat{g}$ and $\hat{b}$, the antenna can be characterized over frequency aiming to widen its radiation performance around its center/design frequency (i.e., for wideband FPCs) or to repeat it at different frequencies (i.e., for multiband FPCs) keeping the same cavity height. Indeed, a thick PRS can be formed using more complex structures (e.g., dielectric-slab-spaced metallic FSSs as in [26] and [27]), requiring more complicated frequency dispersion of $\hat{g}$ and $\hat{b}$ which indeed lead to wideband and multiband FPCs.

V. Analytical Versus Numerical Results

A. Formulas Against Full-Wave Results

In this section, using numerical simulations (i.e., FW calculations carried-out using the finite element method by Ansys HFSS) the accuracy of the proposed formulas is investigated. The unit-cell of a desired PRS is surrounded by periodic boundaries modeling an infinitely extended PRS along its plane. The PRS unit-cell is linked to two waveports on the top and the bottom which along with periodic boundaries, model the plane-wave illumination on the PRS. Finally, reflected and transmitted fields are derived and the scattering parameters are de-embedded to the reference sections chosen to be the upper and lower surfaces of the PRS (these calculations are carried-out using the finite element method by Ansys HFSS). The upward admittance is found using the two-port network modeling the $Y_{\text{up}} = Y_0(\hat{g} + j\hat{b}) = Y_{11} - Y_{21}Y_{12}/(Y_0 + Y_{22})$, where Y_{11}, Y_{12}, Y_{21}, and Y_{22} are the elements of the Y-matrix. As an example, five FPC antennas are designed to resonate at 60 GHz. Five different FSSs with the same unit-cell-size (2×2 mm^2), are designed made of rectangular periodic holes, with length and width of $L \times W$ (hence, the period is $U = 2$ mm in each direction). Fig. 2 shows the normalized conductance and susceptance model of the designed FSSs for various thickness of the FSS at 60 GHz.

Looking at Fig. 2, for thin metallic FSS layers, $\hat{g} \cong 1$ and this value decreases as the thickness of the FSS increases. Table I shows the

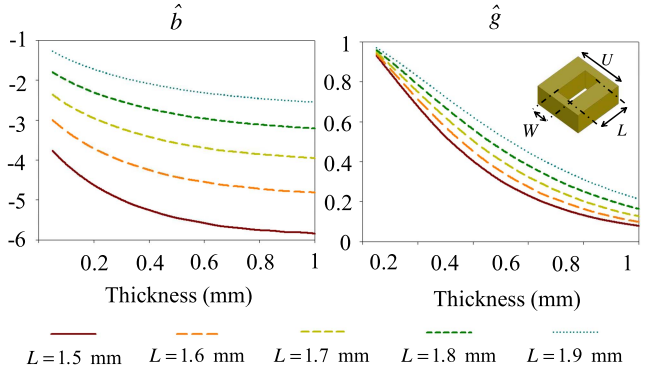

Fig. 2. Normalized equivalent conductance and susceptance of a thick metallic FSS as a function of the thickness $t$of the FSS.

TABLE I

FPC ANTENNAS FORMED BY THICK METALLIC FSS. PROPOSED FORMULAS (7), (10), AND (14) COMPARED AGAINST FW RESULTS

$L\times W$ mm^2	$\hat{b}$	$\hat{g}$	h (mm) Eq.(3)	Dir. (dB) Eq.(10) FW	GBW (%) - FW	PBW (%) Eq.(6) FW	FOM Eq.(14) FW
1.5×1	5.5	0.31	2.36	25.8 26.7	0.65	0.65 0.60	2.47 2.8
1.6×1	4.4	0.36	2.32	23.2 24.2	1.0	1.18 0.9	2.47 2.4
1.7×1	3.6	0.41	2.28	20.9 21.2	1.9	2.01 1.5	2.47 2.0
1.8×1	2.9	0.47	2.23	18.4 19.0	2.9	3.56 2.3	2.47 1.8
1.9×1	2.2	0.53	2.16	15.5 16.3	5.0	6.97 4.0	2.47 1.7

$\hat{g}$ and $\hat{b}$ values, modeling each of the designed FSSs with the chosen thickness of $t = 0.5$ mm, as well as the values of directivity (10), and broadside PBW (6), for such cases obtained by our proposed formulas. The formula for PBW (6) leading to the results in Table I is compared with the PBW obtained by solving (5) numerically for $\omega_{3\text{ dB}}^{\pm}$, or analogously by plotting (2) versus frequency. In these calculation, we account for the frequency dependency of $\hat{g}$ and $\hat{b}$, leading to a PBW of 0.63%, 1.1%, 1.8%, 3.0%, and 5.1%, for directivity cases in descending order, respectively. These values are in good agreement with the proposed formula (6) reported in Table I, valid for highly directive antennas. Indeed the largest error is for the lowest directive case.

Results in Table I are also compared with those obtained by FW analysis. Although this antenna can be fed using planar feeding structures, as proposed in [14], [15], and [20], in the examples discussed here the antenna is excited with a half-a-wavelength slot opening at the center of the ground plane of the antenna. In order to simulate the antenna, as in a realistic scenario, the FPC antenna is truncated laterally using the formulas discussed in [4] and based on the estimated value $\hat{\alpha}$ calculated using (13). Here, in the FW calculations, the FPC is made of a square PRS consisting of 26 element by 26 unit cells (therefore the size is 52 mm × 52 mm) over a 60 mm × 60 mm ground plane.

The FW simulated radiation patterns of the designed antennas, in both E- and H-planes, at their center frequency, i.e., at 60 GHz, are shown in Fig. 3. The simulated radiation efficiency of the designed antennas, as also studied in [28] presenting methods to design highly efficient FPCs formed by thick PRSs, is more than 95% for all cases. Table I shows that results of directivity (Dir.), GBW and broadside

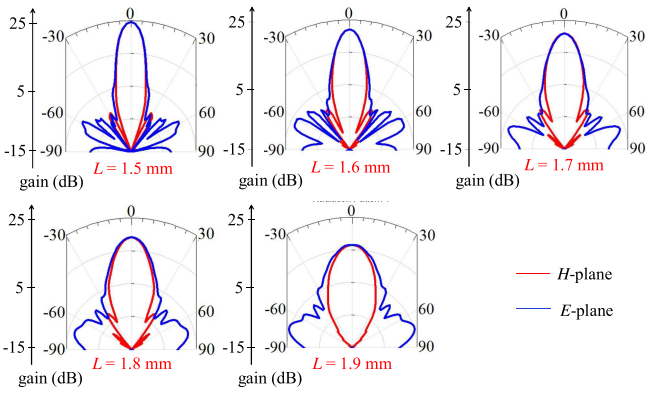

Fig. 3. Simulated radiation patterns, in both E- and H-planes, of the designed antennas shown in Table I at center frequency of 60 GHz.

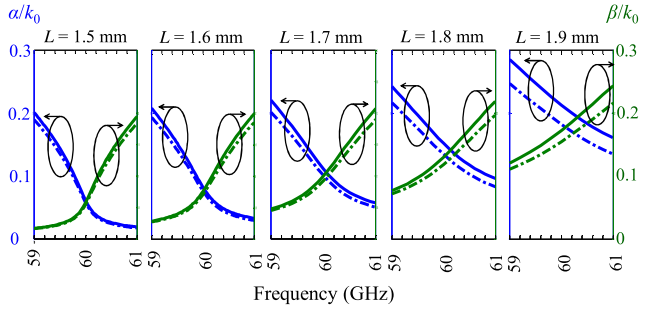

Fig. 4. Dispersion diagram (the attenuation and propagation LW constants for both TE and TM waves versus frequency) for the antennas shown in Table I (all with FSS thickness $t = 0.5$ mm). Note, the dashed and solid lines are representing the TE and TM waves, respectively. TE and TM dispersions tend to coincide with each other for large directivity antennas, i.e., for the cases with smallest values of $\hat{\beta} = \hat{\alpha} = \delta$.

TABLE II

LW CONSTANTS OF THE DESIGNED ANTENNAS IN TABLE I, EVALUATED AT THE OPTIMUM CONDITION, USING NEW FORMULA (13) AND BY SOLVING (11)

L (mm)	$\hat{\alpha}=\hat{\beta}$ using Eq.(13)	$\hat{\alpha}=\hat{\beta}$ (at f_{TE})	$\hat{\alpha}=\hat{\beta}$ (at f_{TM})
1.5	0.06	0.06	0.06
1.6	0.08	0.07	0.08
1.7	0.1	0.1	0.1
1.8	0.135	0.13	0.14
1.9	0.19	0.17	0.19

PBW obtained from FW simulations are in agreement with the values obtained by proposed formulas (6) and (10) for directivity and broadside PBW. FW bandwidths are calculated by looking at plots of gain and broadside power varying with frequency, not shown here for brevity. Moreover, the FoM is calculated using FW values and compared with our proposed formula (14), showing good agreement for the high directivity cases. These results prove that (6) and (10) are good engineering formulas for estimating directivity and PBW without the need of simulating the whole FPS antenna.

B. Leaky-Wave Analysis

Fig. 4 shows the dispersion diagram of the LW attenuation and propagation constants versus frequency, for both dominant TE and TM waves. The LW wavenumbers are found by solving (11) in the frequency range 59–61 GHz, for both TE and TM wave. Table II shows the calculated LW constants of both TE and TM waves by

solving (11) at the optimum condition for each cavity shown in Table I. The LW values obtained from solving (11) are compared to the values estimated using the *new formula* (13), verifying its accuracy.

VI. Conclusion

Novel closed-from formulas are derived characterizing the radiation performance of FPC antennas formed by *thick* arbitrary PRS. These formulas reduce to those previously studied for the case of and FPC with *extremely thin* PRS discussed in [1] and [2]. Numerical calculations verify the accuracy of the new proposed formulas to predict the antenna radiation performance and the LW complex wavenumber. This communication provides a valuable design-tool to design FPC antennas especially at very high frequencies, e.g., at millimeter-waves as in [19] and [20], where the thickness of a partially reflective surface often cannot be neglected or sometimes it is even necessary to guarantee mechanical stability. Note that the formulas shown in this communication provide an estimate of the FPC antenna performance without the need of stimulating the whole structure.

Acknowledgment

The authors would like to acknowledge the support of Ansys Corporation for the use of the simulation software (HFSS).

References

[1] G. Lovat, P. Burghignoli, and D. R. Jackson, "Fundamental properties and optimization of broadside radiation from uniform leaky-wave antennas," *IEEE Trans. Antennas Propag.*, vol. 54, no. 5, pp. 1442–1452, May 2006.

[2] T. Zhao, D. R. Jackson, J. T. Williams, and A. A. Oliner, "General formulas for 2-D leaky-wave antennas," *IEEE Trans. Antennas Propag.*, vol. 53, no. 11, pp. 3525–3533, Nov. 2005.

[3] D. R. Jackson and N. G. Alexopoulos, "Gain enhancement methods for printed circuit antennas," *IEEE Trans. Antennas Propag.*, vol. 33, no. 9, pp. 976–987, Sep. 1985.

[4] R. Gardelli, M. Albani, and F. Capolino, "Array thinning by using antennas in a Fabry–Perot cavity for gain enhancement," *IEEE Trans. Antennas Propag.*, vol. 54, no. 7, pp. 1979–1990, Jul. 2006.

[5] T. Zhao, D. R. Jackson, J. T. Williams, H.-Y. D. Yang, and A. A. Oliner, "2-D periodic leaky-wave antennas—Part I: Metal patch design," *IEEE Trans. Antennas Propag.*, vol. 53, no. 11, pp. 3505–3514, Nov. 2005.

[6] T. Zhao, D. R. Jackson, and J. T. Williams, "2-D periodic leaky-wave antennas—Part II: Slot design," *IEEE Trans. Antennas Propag.*, vol. 53, no. 11, pp. 3515–3524, Nov. 2005.

[7] D. R. Jackson *et al.*, "The fundamental physics of directive beaming at microwave and optical frequencies and the role of leaky waves," *Proc. IEEE*, vol. 99, no. 10, pp. 1780–1805, Oct. 2011.

[8] G. Lovat, P. Burghignoli, F. Capolino, and D. R. Jackson, "Highly-directive planar leaky-wave antennas: A comparison between metamaterial-based and conventional designs," in *Proc. Eur. Microw. Assoc.*, Mar. 2006, pp. 12–21.

[9] H. Ostner, E. Schmidhammer, J. Detlefsen, and D. R. Jackson, "Radiation from dielectric leaky-wave antennas with circular and rectangular apertures," *Electromagnetics*, vol. 17, pp. 505–535, Jan. 1997.

[10] R. Sauleau, P. Coquet, T. Matsui, and J.-P. Daniel, "A new concept of focusing antennas using plane-parallel Fabry–Perot cavities with nonuniform mirrors," *IEEE Trans. Antennas Propag.*, vol. 51, no. 11, pp. 3171–3175, Nov. 2003.

[11] Y. Lee, X. Lu, Y. Hao, S. Yang, J. R. G. Evans, and C. G. Parini, "Low-profile directive millimeter-wave antennas using free-formed three-dimensional (3-D) electromagnetic bandgap structures," *IEEE Trans. Antennas Propag.*, vol. 57, no. 10, pp. 2893–2903, Oct. 2009.

[12] S. J. Franson and R. W. Ziolkowski, "Gigabit per second data transfer in high-gain metamaterial structures at 60 GHz," *IEEE Trans. Antennas Propag.*, vol. 57, no. 10, pp. 2913–2925, Oct. 2009.

[13] Y. Coulibaly, M. Nedil, L. Talbi, and T. A. Denidni, "Design of high gain and broadband antennas at 60 GHz for underground communications systems," *Intl. J. Antennas Propag.*, vol. 2012, Jan. 2012, Art. no. 386846.

[14] S. A. Hosseini, F. Capolino, and F. De Flaviis, "Q-band single-layer planar Fabry–Pérot cavity antenna with single integrated-feed," *Prog. Electromagn. Res. C*, vol. 52, pp. 135–144, Aug. 2014.

[15] A. Hosseini, F. De Flaviis, and F. Capolino, "A 60 GHz simple-to-fabricate single-layer planar Fabry–Pérot cavity antenna," *IET Microw., Antennas Propag.*, vol. 9, no. 4, pp. 313–318, Mar. 2015.

[16] S. A. Hosseini, F. Capolino, and F. De Flaviis, "A new formula for the pattern bandwidth of Fabry–Pérot cavity antennas covered by thin frequency selective surfaces," *IEEE Trans. Antennas Propag.*, vol. 59, no. 7, pp. 2724–2727, Jul. 2011.

[17] S. A. Hosseini, F. Capolino, F. De Flaviis, P. Burghignoli, G. Lovat, and D. Jackson, "Improved method to estimate the 3 dB power bandwidth of a Fabry–Pérot cavity antenna covered by a thin frequency selective surface," in *Proc. IEEE Int. Symp. Antennas Propag.*, Spokane, WA, USA, Jul. 2011, pp. 1281–1284.

[18] A. Hosseini, F. Capolino, F. De Flaviis, P. Burghignoli, G. Lovat, and D. R. Jackson, "Improved bandwidth formulas for Fabry–Pérot cavity antennas formed by using a thin partially-reflective surface," *IEEE Trans. Antennas Propag.*, vol. 62, no. 5, pp. 2361–2367, May 2014.

[19] S. A. Hosseini, F. Capolino, and F. De Flaviis, "Design of a single-feed all-metal 63 GHz Fabry–Perot cavity antenna using a TL and a wideband circuit model," in *Proc. IEEE Int. Symp. Antennas Propag.*, Charleston, SC, USA, Jun. 2009, pp. 1–4.

[20] A. Hosseini, F. Capolino, and F. De Flaviis, "Gain enhancement of a V-band antenna using a Fabry–Pérot cavity with a self-sustained all-metal cap with FSS," *IEEE Trans. Antennas Propag.*, vol. 63, no. 3, pp. 909–921, Mar. 2015.

[21] F. Costa and A. Monorchio, "Design of subwavelength tunable and steerable Fabry–Perot/leaky wave antennas," *Prog. Electromagn. Res.*, vol. 111, pp. 467–481, 2011.

[22] Y. Ge and W. Can, "Efficient characterization of Fabry–Perot resonator antennas," in *Proc. Prog. Electromagn. Res. Symp.*, Taipei, Taiwan, Mar. 2013, pp. 905–909.

[23] L. B. Felsen and N. Marcuvitz, *Radiation and Scattering of Waves*, 2nd ed. New York, NY, USA: Wiley, 2003.

[24] P. Burghignoli, G. Lovat, F. Capolino, D. R. Jackson, and D. R. Wilton, "Directive leaky-wave radiation from a dipole source in a wire-medium slab," *IEEE Trans. Antennas Propag.*, vol. 56, no. 5, pp. 1329–1339, May 2008.

[25] C. A. Balanis, *Antenna Theory: Analysis and Design*, 2nd ed. New York, NY, USA: Wiley, 1997.

[26] Y.-F. Lu and Y.-C. Lin, "Design and implementation of broadband partially reflective surface antenna," in *Proc. IEEE AP-S Symp.*, Spokane, WA, USA, Jul. 2011, pp. 2250–2253.

[27] Y. Ge, K. P. Esselle, and T. S. Bird, "The use of simple thin partially reflective surfaces with positive reflection phase gradients to design wideband, low-profile EBG resonator antennas," *IEEE Trans. Antennas Propag.*, vol. 60, no. 2, pp. 743–750, Feb. 2012.

[28] S. F. Mahmoud and Y. M. M. Antar, "Study of surface waves on planar high gain leaky wave antennas," in *Proc. IEEE Int. Symp. Antennas Propag.*, Toronto, ON, Canada, Jul. 2010, pp. 1–4.